Inorganic Chemistry

Article

pubs.acs.org/IC

# Reinvestigation of $Np_2Se_5$: A Clear Divergence from $Th_2S_5$ and $Th_2Se_5$ in Chalcogen−Chalcogen and Metal−Chalcogen Interactions

Geng Bang Jin,*[,†,‡] Yung-Jin Hu,[†] Brian Bellott,[‡] S. Skanthakumar,[†] Richard G. Haire,[§] L. Soderholm,[†] and James A. Ibers[‡]

[†]Chemical Sciences and Engineering Division, Argonne National Laboratory, Argonne, Illinois 60439, United States

[‡]Department of Chemistry, Northwestern University, Evanston, Illinois, 60208-3113, United States

[§]Chemical Sciences Division, Oak Ridge National Laboratory, Oak Ridge, Tennessee 37831, United States

Supporting Information

**ABSTRACT:** Single crystals of $Np_2Se_5$ have been prepared through the reactions of Np and Se at 1223 K in an $Sb_2Se_3$ flux. The structure of $Np_2Se_5$, which has been characterized by single-crystal X-ray diffraction methods, crystallizes in the tetragonal space group $P4_2/nmc$. The crystallographic unit cell includes one unique Np and two Se positions. Se(1) atoms form one-dimensional infinite chains along the *a* and *b* axes with alternating intermediate Se−Se distances of 2.6489 (8) and 2.7999 (8) Å, whereas Se(2) is a discrete $Se^{2-}$ anion. Each Np is coordinated to 10 Se atoms and every $NpSe_{10}$ polyhedron shares faces, edges, or vertices with 14 other identical metal polyhedra to form a complex three-dimensional structure. Np $L_{III}$-edge X-ray Absorption Near Edge Structure (XANES) measurements show a clear shift in edge position to higher energies for $Np_2Se_5$ compared to $Np_3Se_5$ ($Np^{3+}{}_2Np^{4+}Se^{2-}{}_5$). Magnetic susceptibility measurements indicate that $Np_2Se_5$ undergoes a ferromagnetic-type ordering below 18(1) K. Above the transition temperature, $Np_2Se_5$ behaves as a paramagnet with an effective moment of 1.98(5) $\mu_B$/Np, given by a best fit of susceptibilities to a modified Curie−Weiss law over the temperature range 50−320 K.

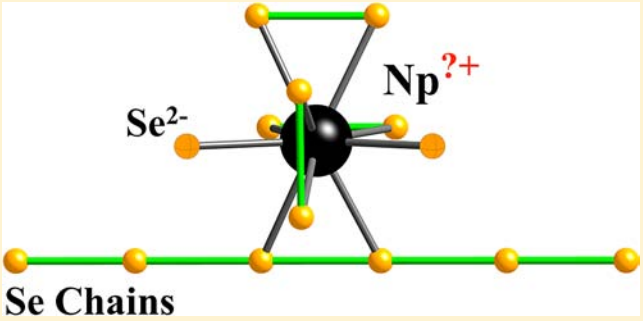


## INTRODUCTION

When compared to the oxides, halides, and pnictides, binary actinide chalcogenides $An_xQ_y$ (An = actinide; Q = S, Se, Te) have a broader chemical composition and structural variety, exhibiting An:Q ratios between 1:1 and 1:5.[1] Underpinning this variety are the redox and bonding capabilities of the chalcogens, which enable the formation of a variety of Q−Q interactions.[2−7] Depending on specifics of the metal (M) sublattice, these interactions permit the formation of a host of discrete chalcogenide monomers, finite oligomers, one-dimensional chains, ribbons, two-dimensional layers, or three-dimensional networks. This is particularly true for the selenides and tellurides.[7] The formation of oligomeric moieties is accompanied by the reduction of neutral Q to $Q^{x-}$ ($0 < x \leq 2$) anions. Depending on the redox potential of the cation, there is an added potential for variability through in situ redox reactions with charge transfer between the M and Q substructures.

Actinide compounds display extremely rich chemistry owing to their partially filled 5f orbitals with varying degrees of localization that increase across the series.[1] A long discussed issue in the field of actinide materials is the bonding or itinerancy of 5f electrons and the resulting f counts or valences of the metal ions. Clues to the electron distribution within chalcogenide compounds can be found in their structural details, specifically in the An−Q and Q−Q distances obtained from single-crystal studies, because these distances are known to scale with An and Q valences.[7,8] Neptunium (Np) is particularly important in this regard, as it sits on the border between tetravalent thorium (Th), uranium (U), and more lanthanide-like plutonium (Pu), exhibiting an intermediate behavior in the $An_xQ_y$ system.[9] More than half of reported $Np_xQ_y$ compounds, including $Np_3Q_5$ (Q = S, Se),[10] $\beta$-$NpS_2$,[11] $Np_2Q_5$ (Q = S, Se),[12,13] $NpQ_3$ (Q = S, Se),[14−16] are isostructural with Th or U analogues, within which Np is predominantly +4; $Np_2Q_3$ (Q = S, Se, Te),[11,14,15,17] $NpTe_2$,[17] and $NpTe_3$[17] are isostructural with Pu analogues, within which Np is +3; NpQ (Q = S, Se, Te) are isostructural with both U and Pu phases adopting the NaCl-type structure at ambient conditions.[18] However many of the $Np_xQ_y$ compounds were studied a few decades ago using powder samples. As a result, ambiguities remain about selected crystal structures and physical properties, and even the existence of some of the reported phases, owing largely to impurities in the powder samples and the lack of single-crystal data.[9,18]

**Received:** May 31, 2013
**Published:** July 24, 2013

   dx.doi.org/10.1021/ic401384t | *Inorg. Chem.* 2013, 52, 9111−9118

As part of broader research efforts to understand electron distributions in redox-active 5f systems we are interested in clarifying the structures and electron distributions in some $Np_xQ_y$ phases. Toward this end we have successfully prepared large single crystals of mixed-valent $Np_3Q_5$ (Q = S, Se; $Np^{3+}{}_2Np^{4+}Q^{2-}{}_5$) compounds and characterized their structures and magnetism.[10] In the current study, we focus on the series of $An_2Q_5$ (An = Th, U, Np; Q = S, Se, Te).[12−14,19−23] Previous single-crystal studies have shown that the pseudotetragonal structure of $Th_2S_5$ contains $S^{2-}$ and $S_2^{2-}$ anions and $Th^{4+}$ cations,[21] whereas the structure of $U_2Te_5$ consists of infinite $-Te-Te-Te^{x-}-$ chains ($0 < x < 2$), rendering the valence state of U ambiguous.[24,25] $Th_2Se_5$, $U_2S_5$, $Np_2S_5$, and $Np_2Se_5$ were considered to be isostructural with $Th_2S_5$ including the $Q^{2-}$, $Q_2^{2-}$, and $An^{4+}$ ions; however, their X-ray powder diffraction patterns did not display the split reflections observed for $Th_2S_5$. The splittings seen in the Th analogue suggest a symmetry lower than tetragonal.[13,22] Single-crystal X-ray diffraction data of $Th_2Se_5$ have been recently reported, where a modulated structure was determined, crystallizing in a monoclinic superspace group.[23] Furthermore, the $^{237}Np$ Mössbauer spectrum on a powder sample of $Np_2Se_5$ showed an isomer shift intermediate to those for the $Np^{4+}$ and $Np^{3+}$ chalcogenides.[13] To our knowledge, "$U_2Se_5$", "$Th_2Te_5$", and "$Np_2Te_5$" have not yet been reported.[20] Considering this information, together with the different chemistry and ionic radii observed among $An_xQ_y$ (An = Th, U, Np; Q = S, Se, Te) systems, the chemical bonding and structures within $U_2S_5$, $Np_2S_5$, and especially $Np_2Se_5$ could be different from those of $Th_2S_5$, $Th_2Se_5$, and $U_2Te_5$.

Herein we report a high-yield synthesis of $Np_2Se_5$, its single-crystal structure, X-ray absorption spectra, and magnetic properties. The focus of the structural work lies on the Se sublattice and whether it shows the same Q−Q interactions as those seen for $Th_2S_5$ and $Th_2Se_5$, which would indirectly confirm the Np valence state. Our studies show that the structure of $Np_2Se_5$ is related to, but deviates from those of $Th_2S_5$ and $Th_2Se_5$. The implications of this difference are examined in terms of different Q−Q and An−Q interactions, and ionic radii. XANES and magnetic susceptibility data are included to complement the structural findings. Taken together, our results provide evidence that the valence state of Np in $Np_2Se_5$ is greater than +4 and probably less than +4.

## EXPERIMENTAL METHODS

**Syntheses.** Se (Cerac, 99.999%) and Sb (Aldrich, 99.5%) were used as received. Brittle $^{237}Np$ chunks were crushed and used as provided (ORNL). $Sb_2Se_3$ was prepared from the direct reaction of the elements in a sealed fused-silica tube at 1123 K.[26]

***Caution!*** *$^{237}Np$ is an α- and γ-emitting radioisotope and as such is considered a health risk. Its use requires appropriate infrastructure and personnel trained in the handling of radioactive materials.* The procedures we use for the syntheses of Np compounds have been described.[27] Np (0.020 g, 0.084 mmol), Se (0.020 g, 0.253 mmol), and $Sb_2Se_3$ (0.100 g, 0.208 mmol) were loaded into fused-silica ampules in an Ar-filled glovebox and then flame-sealed under vacuum. The reaction mixtures were heated in a furnace to 1173 K in 24 h, then to 1223 K in 24 h, kept at 1223 K for 48 h, cooled to 1173 K in 24 h, then cooled to 673 K in 150 h, and finally cooled to 298 K in 24 h. The reaction products included black crystals of $Np_2Se_5$ and unreacted black lustrous $Sb_2Se_3$[28] crystals in the form of large clusters. The separation of the flux from the products was achieved by slightly tilting the furnace, which caused the flux to flow to the bottom of the ampules leaving the products behind, making manual separation with the aid of a stereomicroscope feasible. Only diffraction peaks from $Np_2Se_5$ were found in the X-ray powder diffraction pattern of the remaining solid.

**Structure Determination.** Single-crystal X-ray diffraction data for $Np_2Se_5$ at 100 K were collected with the use of graphite-monochromatized MoKα radiation ($\lambda$ = 0.71073 Å) on a Bruker APEX2 diffractometer.[29] The crystal-to-detector distance was 5.106 cm, and data were collected by a scan of 0.3° in $\omega$ in groups of 606 frames at $\varphi$ settings of 0°, 90°, 180°, and 270°. The exposure time was 30 s/frame. The collection of intensity data as well as cell refinement and data reduction were carried out with the use of the program APEX2.[29] Precession pictures, generated with APEX2 software, showed only the expected symmetry and systematic absences. There was no evidence of modulation or of splitting of the high-order reflections.

Absorption corrections, as well as incident beam and decay corrections, were performed with the use of the program SADABS.[30] The structure was solved with the direct-methods program SHELXS and refined with the least-squares program SHELXL.[31] The final refinement included anisotropic displacement parameters. The program STRUCTURE TIDY[32] was used to standardize the positional parameters. Additional experimental details are given in Table 1 and the Supporting Information.

**Table 1. Crystal Data and Structure Refinement for $Np_2Se_5$**

| | |
|---|---|
| Fw | 868.80 |
| crystal system | tetragonal |
| $Z$ | 2 |
| $a$ (Å) | 5.4488(3) |
| $c$ (Å) | 10.6428(7) |
| $V$ (Å$^3$) | 315.98(3) |
| $T$ (K) | 100(2) |
| $\rho_c$ (g/cm$^3$) | 9.131 |
| $\mu$ (cm$^{-1}$) | 613.65 |
| $R(F)^a$ | 0.0188 |
| $R_w(F_o^2)^b$ | 0.0427 |

$^aR(F) = \sum||F_o| - |F_c||/\sum|F_o|$ for $F_o^2 > 2\sigma(F_o^2)$. $^bR_w(F_o^2) = \{\sum[w(F_o^2 - F_c^2)^2]/\sum wF_o^4\}^{1/2}$ for all data; $w^{-1} = \sigma^2(F_o^2) + (qF_o^2)^2$ for $F_o^2 \geq 0$; $w^{-1} = \sigma^2(F_o^2)$ for $F_o^2 < 0$; $q$ = 0.0216.

**X-ray Powder Diffraction.** X-ray powder diffraction patterns were collected with a Scintag X1 diffractometer using Cu Kα radiation ($\lambda$ = 1.5418 Å). The powder sample was loaded into an encapsulated container with Kapton windows, curved to minimize the X-ray absorption by the Kapton.

**X-ray Absorption Near Edge Structure (XANES) Experiments of $Np_3Se_5$ and $Np_2Se_5$.** Approximately 2 mg each of $Np_3Se_5$ and $Np_2Se_5$ were used to prepare samples for XANES measurements. Neptunium samples were finely ground in a mortar and pestle with an appropriate amount of inert diluent. Sample mixtures were loaded in 0.8 mm thick polypropylene holders, and these were further contained by two layers of Kapton tape before being placed into a purpose-built actinide-sample container for measurements on the synchrotron beamline. Np $L_{III}$-edge X-ray absorption spectra (XAS) were collected at 298 K at the APS on bending magnet beamline 12-BM-B, which is equipped with a Si (111) double-crystal monochromator, a flat energy discriminating 22 keV cutoff mirror, and a toroidal (beam focusing) Rh-coated Pt mirror. Data were collected in transmission mode. Ion chambers were filled with Ar gas. The monochromator energy was calibrated by measuring a Zr metal foil between sample scans and setting the first inflection point of the derivative spectrum to 17998.0 eV.[33] The data were reduced and normalized following standard procedures.[34]

Measured X-ray absorption spectra were pre-edge subtracted and normalized to unit edge-step using SIXPack,[35] a graphical user interface front-end to the IFEFFIT XAS analysis package.[36] The second derivative of the Np absorption edge spectra were numerically


dx.doi.org/10.1021/ic401384t | Inorg. Chem. 2013, 52, 9111−9118

calculated and smoothed using a binomial smoothing filter to remove high frequency noise.[37]

**Magnetic Susceptibility Measurements.** Magnetic susceptibility data were collected on 6.2 mg of powdered single crystals of $Np_2Se_5$ with the use of a Quantum Design MPMS 7 SQUID magnetometer. The empty sample holder was measured separately, and the signal was subtracted directly from the magnetic response. Variable field measurements were performed at 2, 10, 15, 20, 50, and 300 K to a maximum of 5 T. Variable temperature experiments were carried out between 5 and 320 K, under applied fields of 0.01, 0.05, 0.2, and 0.5 T; these provided the same results within experimental error.

## RESULTS

**Syntheses.** Preparations of powder samples of $An_2Se_5$ (An = Th, Np) have been previously reported, including direct reactions between An/$AnH_x$ and Se, or thermal decomposition of $AnSe_3$.[13,19,22] Single crystals of $Np_2Se_5$ were first obtained from the reaction of Np, $P_2Se_5$, and Se in a molar ratio of 2:3:20 at 1173 K.[38] Rational synthesis of $Np_2Se_5$ from the elements was achieved using an $Sb_2Se_3$ flux (mp 884 K). Excess Se was added to ensure a complete reaction of Np. $Th_2Se_5$ has been synthesized in a similar manner and has been found as a byproduct in many thorium selenide reactions.[23,39] In contrast, numerous attempts to prepare "$U_2Se_5$" have failed.[39] These observations indicate different stabilities of $An_2Se_5$ (An = Th, U, Np), assuming the compound "$U_2Se_5$" even exists.

$Sb_2Se_3$ flux has been successfully employed to synthesize a number of lanthanide selenide single crystals, including $Ln_3LuSe_6$ (Ln = La, Ce),[26] $Gd_{1.05}Sc_{0.95}Se_3$,[40] and $EuLn_2Se_4$ (Ln = Tb–Lu).[41] Recently it was used to prepare a lanthanide/actinide selenide ($U_2La_2Se_9$) in a near quantitative yield.[42] In the current study, the $Np_2Se_5$ was prepared in the same flux. Clearly $Sb_2Se_3$ flux shows great potential for syntheses of lanthanide and actinide selenides.

**Structure.** The structure of $Np_2Se_5$ was examined earlier by X-ray powder diffraction methods.[13] The diffraction lines were indexed in an orthorhombic, pseudotetragonal unit cell ($a$ = 7.725(3) Å, $b$ = 7.725(3) Å, and $c$ = 10.622(5) Å) because $Np_2Se_5$ was considered to be isostructural with $Th_2S_5$, even though there was no evidence for a splitting of reflections similar to that found in $Th_2S_5$.[13,22] In the current single-crystal X-ray diffraction data of $Np_2Se_5$ there was no evidence of either modulation (as in $Th_2Se_5$)[23] or of splitting of the high order reflections (as in $Th_2S_5$).[21] The tetragonal space group $P4_2/nmc$ was determined unambiguously, and the structure was solved in a straightforward manner.

As shown in Figure 1, the tetragonal structure of $Np_2Se_5$ contains one crystallographically unique Np and two Se positions with the site symmetries of 2*mm*. (Np), .*m*. (Se(1)), and $\bar{4}m2$ (Se(2)). Se(1) atoms form one-dimensional infinite chains along $a$ and $b$ axes with alternating intermediate Se–Se distances (Figure 1b). Se(2) is an isolated $Se^{2-}$ anion with closest Se–Se distances of 3.4391(3) Å, too long to have any significant interactions. The Np atom is coordinated to eight Se(1) and two Se(2) atoms (Figure 2). Each $NpSe_{10}$ polyhedron shares two Se(1) and one Se(2) vertices with each of four closest identical neighbors with Np–Np distances of 4.4111(3) Å. Furthermore, it shares one Se(1) edge with each of another eight units and a Se(2) corner with each of two other units with Np–Np distances ranging from 4.9917(4) to 5.4488(3) Å.

Selected interatomic distances for $Np_2Se_5$ are listed in Table 2. The Np–Se distances range from 2.9284(2) to 3.0686(3) Å.

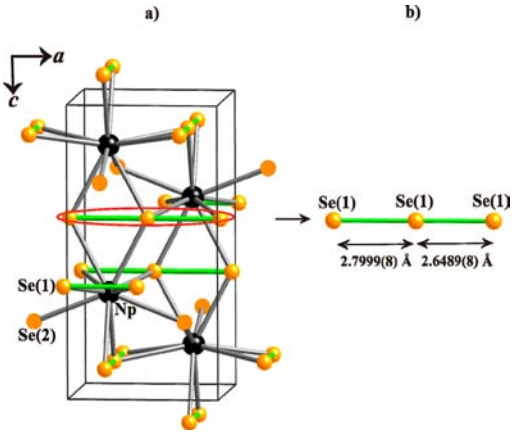


**Figure 1.** (a) Tetragonal unit cell of $Np_2Se_5$ in space group of $P4_2/nmc$. There are one-dimensional linear selenide chains along the $a$ and $b$ axes. Se–Se bonds within the chains are highlighted in green and one of the chains is circled in red; (b) A fragment of an infinite Se(1) chain with alternating long and short Se–Se distances.

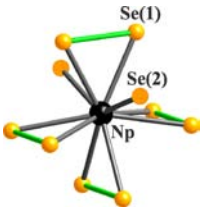


**Figure 2.** Local coordination environment of Np in $Np_2Se_5$.

**Table 2. Selected Interatomic Distances (Å) for $Np_2Se_5$**

| | |
|---|---|
| Np(1)–Se(1) × 2 | 2.9861(4) |
| Np(1)–Se(1) × 2 | 3.0270(4) |
| Np(1)–Se(1) × 4 | 3.0686(3) |
| Np(1)–Se(2) × 2 | 2.9284(2) |
| Se(1)–Se(1) | 2.6489(8) |
| Se(1)–Se(1) | 2.7999(8) |
| Np(1)–Np(1)[a] | 4.4111(3) |

[a]Between two face-shared $NpSe_{10}$ polyhedra.

Other Np–Se distances reported from single-crystal studies for both $Np^{3+}$ and $Np^{4+}$ cations in various coordination environments are tabulated in Table 3. In the compounds $NpCuSe_2$,[43] $Np_3Se_5$,[10] and NpOSe,[44] each Np cation is only coordinated by isolated $Se^{2-}$ anions, whereas in $NpSe_3$,[16] $Np_2Se_5$, and $ANp_2Se_6$ (A = K, Cs)[45] some of the Se atoms connecting to the Np atom engage in additional bonding with each other to form (Se–Se) dimers. The formal coordination numbers of Np atoms in $NpSe_3$,[16] $Np_2Se_5$, and $ANp_2Se_6$[45] are 8, 10, and 8, respectively; however if the (Se–Se) dimer is considered as one large ligand and is replaced with a point at its center, then Np atoms in these compounds are all six-coordinate. This depiction of the bonding would render questionable comparisons of Np–Se distances among $Np_2Se_5$ and other compounds in Table 3. Se(1)–Se(1) distances within the infinite chains are 2.6489(8) and 2.7999(8) Å, which are longer than the typical values of approximately 2.36 Å for a single Se–Se bond,[46] but are significantly shorter than their van der Waals contact (3.88 Å).[47] These distances are slightly shorter than the corresponding values found for similar selenide chains in $AAn_2Se_6$ (A = K, Rb, Cs; An = Th, U, Np), for example, 2.698(3) and 2.924(3)


dx.doi.org/10.1021/ic401384t | Inorg. Chem. 2013, 52, 9111–9118

**Table 3. Comparison of Interatomic Distances (Å) Among Known Neptunium Selenides**

| compound | oxidation state | coordination number | Np−$Se^{2-}$ | Np−(Se−Se) | Se−Se around Np | reference |
|---|---|---|---|---|---|---|
| $NpCuSe_2$ | +3 | 7 | 2.9330(6)−3.1419(6) | | | 43 |
| $Np_3Se_5$ | +3 | 8 | 2.9922(5)−3.1522(5) | | | 10 |
| $Np_3Se_5$ | +4 | 7 | 2.7738(5)−2.9770(7) | | | 10 |
| NpOSe | +4 | 9 ($4O^{2-}$ + $5Se^{2-}$) | 3.0055(5)−3.077(1) | | | 44 |
| $NpSe_3$ | +4 | 8 ($4Se^{2-}$ + 2(Se−Se)) | 2.866(2)−2.927(3) | 2.859(2), 2.876(2) | 2.340(3) | 16 |
| $Np_2Se_5$ | ? | 10 ($2Se^{2-}$ + 4(Se−Se)) | 2.9284(2) | 2.9861(4)−3.0686(3) | 2.6489(8), 2.7999(8) | this work |
| $KNp_2Se_6$ | ? | 8 ($4Se^{2-}$ + 2(Se−Se)) | 2.8673(9), 2.9443(6) | 2.9048(7) | 2.681(2) | 45 |
| $CsNp_2Se_6$ | ? | 8 ($4Se^{2-}$ + 2(Se−Se)) | 2.869(2), 2.9367(9) | 2.898(1) | 2.647(3) | 45 |

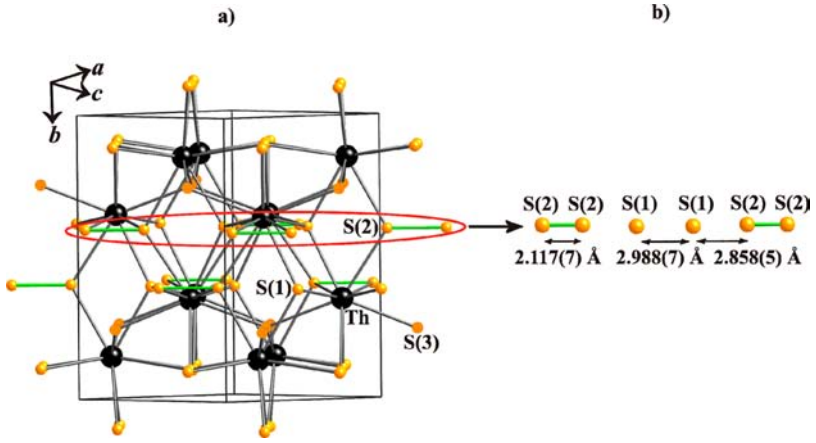


**Figure 3.** Orthorhombic unit cell of $Th_2S_5$ that is twice as large as that of $Np_2Se_5$.[21] The compound crystallizes in space group *Pcnb*. S−S bonds are highlighted in green. One of the S−S chains, which corresponds to the Se(1) chains in $Np_2Se_5$, is circled in red. (b) A fragment of a distorted sulfide chain with discrete $S(1)^{2-}$ anions and $S(2)_2^{2-}$ dimers.

Å in $CsTh_2Se_6$, 2.698(3) and 2.854(3) Å in $RbU_2Se_6$, and 2.681(2) and 2.844(2) Å in $KNp_2Se_6$.[45]

**Comparisons of $Np_2Se_5$, $Th_2S_5$, and $Th_2Se_5$.** The relationship among the tetragonal, orthorhombic, and monoclinic structures of $Np_2Se_5$, $Th_2S_5$, and $Th_2Se_5$, respectively, has been briefly discussed.[22,23] Although these three structures are highly related, they have distinct chalcogen−chalcogen (Q−Q) connectivities. The corresponding Se(1) site that forms linear chains in the $Np_2Se_5$ structure splits into two crystallographically unique S(1) and S(2) positions in the $Th_2S_5$ structure, which results in a lowering of the overall symmetry (Figures 1 and 3). S(1) atoms exist as discrete $S^{2-}$ anions with S−S distances of 2.858(5) and 2.988(7) Å with neighboring S atoms that are too long to have any significant interactions. S(2) atoms form $S_2^{2-}$ dimers with a reasonable S−S single bond distance of 2.117(7) Å (Figure 3).[21] The related $Th_2Se_5$ structure is modulated and contains Se oligomers with a wide distribution of Se−Se distances ranging from 2.447 (5) to 2.967(7) Å. Therefore Q−Q connectivities in $An_2Q_5$ become increasingly more modular in the order of $Np_2Se_5$, $Th_2Se_5$, and $Th_2S_5$. A similar behavior of the chalcogenide sublattice has been observed in the series of $AAn_2Q_6$ (A = K, Rb, Cs, Tl; An = La, Th, U, Np; Q = S, Se) depending on the choice of A, An, and Q.[4,45,48,49] For example, $KU_2Se_6$ contains linear Se chains with two alternating Se−Se distances,[49] $CsNp_2Se_6$ includes a series of Se oligomers,[45] and $K_{0.91}U_{1.79}S_6$, which charge balances with $U^{4+}$, displays $S^-$ and $S_2^{2-}$ species.[49] It should be emphasized that there is no evidence of nonstoichiometry or modulation in the present study of $Np_2Se_5$.

**XANES of $Np_3Se_5$ and $Np_2Se_5$.** Figure 4 shows the comparison between a normalized Np $L_{III}$-edge XANES spectrum, the second derivative of the XANES spectrum for

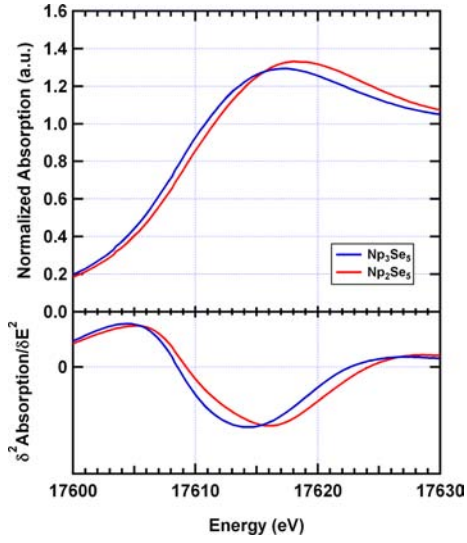


**Figure 4.** Np $L_{III}$-edge XANES (normalized absorbance, top; second derivative, bottom) of $Np_3Se_5$ and $Np_2Se_5$, showing the shift of the $Np_2Se_5$ inflection point to higher energy.

$Np_2Se_5$, and the reference standard $Np_3Se_5$.[10] The absorption edge energies, assigned to the first inflection point of the XANES spectra, are presented in Table 4, where they are compared to edge energies from the literature.[50−52]

Previous structural and $^{237}Np$ Mössbauer spectroscopic studies have inferred that the Np in $Np_3Se_5$ is mixed-valent with crystallographically unique $Np^{3+}$ and $Np^{4+}$ sites in a ratio of 2:1.[10,11] The usual shift in energy between $An^{3+}$ and $An^{4+}$ XANES edges are commonly observed to be approximately 4


dx.doi.org/10.1021/ic401384t | Inorg. Chem. 2013, 52, 9111−9118

**Table 4. XANES Edge Positions (Np $L_{III}$-edge) for Neptunium Selenides**[a,b]

| compound | edge energy (eV) | energy relative to Np metal | reference |
|---|---|---|---|
| $Np_3Se_5$ ($Np_2^{3+}Np^{4+}Se_5$) | 17608.52 | 0.48 | this work |
| $Np_2Se_5$ | 17609.26 | 1.22 | this work |
| Np metal | 17608.04(5) | 0 | 50,51 |
| $Np^{3+}$ in 1 M $HClO_4$ | 17613.8(20) | 5.76 | 52 |

[a]The edge position is defined as the inflection point of the absorption edge or the point where the second derivative of the absorption edge passes through zero. The error in determining the edge energy in this work is 0.14 eV at the 1$\sigma$ level. [b]Neptunium edge energies from the literature are included for comparison.

eV for actinide oxides in solution and the solid state.[53,54] However, the neptunium selenide compounds show a significant shift toward the edge energy of metallic Np when compared to $Np^{3+}$ dissolved in 1 M perchloric acid. Such effects on the edge energy of plutonium selenides have previously been observed,[53] underscoring the need for appropriate reference compounds for XANES determinations of valences. Significant covalent bonding between the Se and the Np may possibly play a role in shifting the absorption edge for this class of compounds to lower energies, which are more characteristic of semiconducting or partially metallic materials.[55] XANES measurements on the two neptunium selenide samples show a 0.7(2) eV shift in edge position to higher energies for the $Np_2Se_5$ compound compared to the $Np_3Se_5$ compound. This shift in edge position indicates an increase in the valence of the Np center in $Np_2Se_5$ as compared to $Np_3Se_5$. Furthermore, the shape of the white-line suggests a rather large bandwidth for the unoccupied 6d density of states, another signature of semiconducting or partially metallic materials.[56,57] We assume an approximate 4.0 eV shift in edge energies between $Np^{3+}$ and $Np^{4+}$, consistent with previous measurements[52] and similar to those previously seen in U and Pu.[53,58] The shift in XANES edge position of $Np_2Se_5$ when compared to that of $Np_3Se_5$ corresponds to an increase in the Np valence of 0.19(5) units. If we set the average valence in $Np_3Se_5$ at 3.33 then we measure the valence of Np in $Np_2Se_5$ to be 3.52(5). Despite the assumptions made to obtain this value and the lack of an appropriate $Np^{4+}$ selenide standard, it is clear from the XANES measurements that the Np valence in $Np_2Se_5$ is greater than +3.

**Magnetism.** The magnetic susceptibility, obtained as a function of temperature under an applied field of 0.01 T, is shown in Figure 5. Highlighted in the inset is the sharp rise in the susceptibility upon cooling that occurs at 18(1) K, a feature indicative of a ferromagnetic-type ordering of the Np moments. The presence of soft ferromagnetism at low temperature, with only a small hysteresis, is supported by the field dependence of the magnetization at low temperature, as revealed in Figure 6. The saturation moment, determined at 0.1 T is 0.87(3) $\mu_B$, a value that continues to rise linearly with increasing field out to the highest field measured, 5.0 T, where it has reached 1.0(2) $\mu_B$. The origin of this slightly increasing moment after saturation has not been studied but would be consistent with a slight canting of the ferromagnetic-moment direction with respect to the principal crystal-field axes.

Above the ordering temperature, the magnetic response is consistent with a simple paramagnet. The data can be described with a modified Curie–Weiss law, appropriate for non-interacting moments, according to

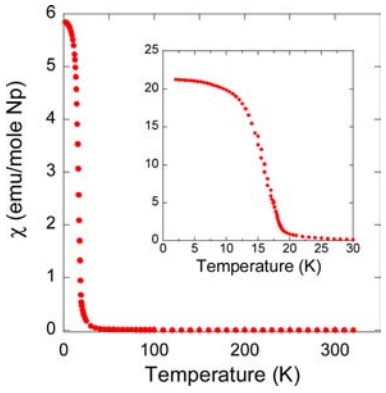


**Figure 5.** Susceptibility of a 6.2 mg sample of $Np_2Se_5$ obtained under an applied field of 0.01 T. The inset shows the same data in the expanded temperature region to highlight the magnetic transition.

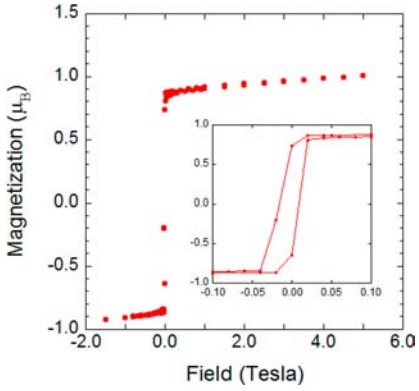


**Figure 6.** Field dependence of the $Np_2Se_5$ magnetization at 2 K is consistent with that seen for a soft ferromagnet, as discussed in the text.

$$\chi_{exp} = \frac{C}{T-\theta} + \chi_{TIP}$$

in which $\theta$, the Weiss constant, considered an indication of the interaction energy between local spins, is expressed as a temperature. This attribution to the origins of $\theta$ can be vitiated by changing populations of crystal-field states with different moments. $\chi_{TIP}$ represents the temperature-independent paramagnetism (TIP) that arises from either itinerant electrons (Pauli paramagnetism) or second-order coupling of crystal-field states (vanVleck paramagnetism). $C$ is the Curie constant and is related to the effective magnetic moment by:

$$\mu_{eff} = \left(\frac{3kC}{N\mu_B^{\,2}}\right)^{1/2}$$

with $k$ as the Boltzmann constant, $N$ as Avogadro's number, and $\mu_B$ the units of Bohr magnetons, equal to $0.927 \times 10^{-20}$ erg/Gauss. A plot of the data as $1/\chi$ versus $T$ is not rectilinear, indicating a significant contribution from the TIP term. A plot of the data as $\chi T$ versus $T$ is also not rectilinear, indicating that within this simple model a Weiss constant is also necessary to reproduce the temperature dependence of the susceptibility.

The best fit to the susceptibility over the temperature range 50–320 K is compared with the data in Figure 7. The Weiss constant determined from the fitting is 21.3(2) K, a value consistent with the onset of ferromagnetic ordering at 18 K suggested by the sharp increase in the susceptibility as the


dx.doi.org/10.1021/ic401384t | Inorg. Chem. 2013, 52, 9111–9118

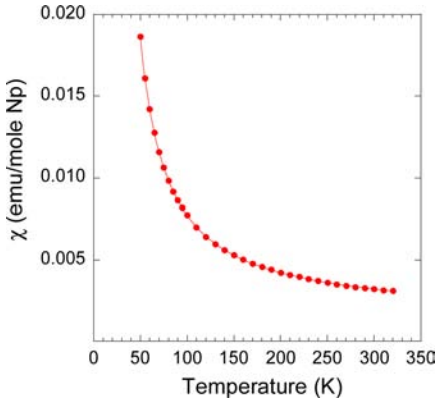


**Figure 7.** Susceptibility of a 6.2 mg sample of $Np_2Se_5$ obtained under an applied field of 0.05 T. The result of the best fit to a modified Curie–Weiss law, shown as the solid line, is $C$ = 0.493(5) emu K/mol, $\theta$ = 21.3(2) K, and $\chi_{TIP}$ = 0.0014(1) emu/mol.

temperature is lowered in that region. The effective moment determined by this fitting method is 1.98(5) $\mu_B$, significantly reduced from the free-ion moment expected for either $Np^{3+}$ (2.68 $\mu_B$) or $Np^{4+}$ (3.62 $\mu_B$). The $\chi_{TIP}$ fit obtained from the data is 0.0014(1) emu/mol.

These results are consistent with and add to previous studies on the magnetic susceptibility of $Np_2Se_5$,[13] notably confirming the low measured effective moment. The moment could be reduced by the electrostatic field imposed by the surrounding ligands (crystal-field effects)[59] or it could be the result of Np–Se interactions that result in intermediate-valence behavior, the latter possibility supported by the larger TIP contribution.[60−62]

## DISCUSSION

**Valence States.** The formula of $Th_2S_5$ can be written as $(Th^{4+})_2(S^{2-})_3(S_2)^{2-}$ because Th is stable only in its tetravalent state and the S–S distances are either within the range for a single bond ($S_2^{2-}$) or too long to be considered to have any interactions ($S^{2-}$). In contrast, the assignment of valence states in $Np_2Se_5$ is more challenging from several perspectives. First among them, Np has two stable valence states in chalcogenide systems, +3 and +4. Second, the Se–Se distances within the linear Se chains are 0.3–0.4 Å longer than a typical single Se–Se bond distance, but there is no routine method to quantify the valence of Se.[7] Third, there are only a limited number of Np–Se distances known from single-crystal studies, and the Np valences are unclear in some of those phases (Table 3). Thus, it is not possible to perform empirical bond-valence calculations to estimate valence states.[63,64]

The $^{237}$Np Mössbauer spectrum obtained from a powder sample of $Np_2Se_5$ showed quadrupole splitting with an isomer shift of 12.7(2) mm $s^{-1}$ relative to $NpAl_2$ at 77 K, which is close to the middle values between those for the $Np^{4+}$-containing and $Np^{3+}$-containing chalcogenides. For example, an isomer shift of −3.2(6) mm $s^{-1}$ and 31.1(3) mm $s^{-1}$ were observed for the $Np^{4+}$ and $Np^{3+}$ sites in $Np_3Se_5$, respectively.[11,13] This suggests that the unique Np in $Np_2Se_5$ may have an intermediate valence between +3 and +4, although where the "+3" isomer shift ends and the "+4" isomer shift begins is not known. Following common usage, intermediate valence is defined as a noninteger valence for a crytallographically unique site.[65]

XANES results from the current study suggest a higher valence than +3 for Np. Considering the charge-balance, the formula can be written as $(Np^{(3+x)+})_2(Se^{2-})(Se_4)^{(4+2x)-}$ ($0 < x \leq 1$). To obtain a reasonable estimate of $x$, a close comparison can be made between $CsTh_2Se_6$[27] and $Np_2Se_5$. Similar to $Np_2Se_5$, the structure of $CsTh_2Se_6$[27] contains two crystallographically unique Se sites. Se(1) is a discrete $Se^{2-}$ anion and Se(2) forms infinite linear chains with alternating Se–Se distances of 2.698(3) and 2.924(3) Å. Charge-balance considerations, based on the formula of $CsTh_2Se_6$ with an atomic ratio Se(1):Se(2) of 1:2, lead to an average oxidation state of −1.25 per Se(2) within the selenide chain. As we described earlier, the Se–Se distances within the selenide chain in $Np_2Se_5$ are slightly shorter than those in $CsTh_2Se_6$, which suggests stronger Se–Se interactions. Distance-valence correlations are interpreted as fewer electrons donated by cations to the p $\sigma^*$ orbitals of Se–Se interactions, giving rise to a higher oxidation state of Se (>−1.25) for $Np_2Se_5$. If we use such a correlation here, then the valence state of Np would be between +3 and +3.5 ($0 < x < 0.5$). Alternatively, if we assume the difference in Se–Se distances between $Np_2Se_5$ and $CsTh_2Se_6$ are within the acceptable range for $Se^{-1.25}$ anions ($x$ = 0.5), then the valence state of Np would be close to +3.5, which is consistent with Mössbauer and XANES results. In different chemical environments, Se–Se distances for the same valence state could vary over an even wider range. Although the bulk of the data point to an intermediate valent Np, the possibility of Np being in its more common +4 valence state in $Np_2Se_5$ cannot be completely ruled out.

**$M_2Q_5$.** Driven by the requirement for charge neutrality, the lanthanide and actinide members of the $M_2Q_5$ series ($Ln_2Te_5$ (Ln = La–Nd, Sm, Gd–Ho, Dy),[66,67] $U_2Te_5$,[24,25] $Np_2Se_5$, $Th_2Se_5$,[23] $Th_2S_5$,[21] and $Np_2O_5$[68]) provide an excellent example of gradually changing electronic structures from metal to insulator as a function of Q–Q and M–Q interactions. The structure of $Ln_2Te_5$ ($Ln^{3+}{}_2(Te^{2-})_2(Te_3)^{2-}$) contains metallic $[Te_3]^{2-}$ two-dimensional sheets where each Te atom connects to four other Te atoms,[67] whereas the telluride layers in $U_2Te_5$ are semiconducting, where each Te atom only bonds to two other Te atoms to form one-dimensional chains.[24,25] These telluride chains in $U_2Te_5$ are similar to the selenide chains in $Np_2Se_5$ but with stronger Q–Q interactions. As described above, the Q–Q chains in $Th_2Se_5$ distort into Se oligomers and further in $Th_2S_5$ into discrete $S_2^{2-}$ and $S^{2-}$ species. The insulator $Np_2O_5$ contains neptunyl ($NpO_2^+$) and $O^{2-}$ ions without any O–O interactions.[21,68] The Q–Q interactions decrease in the order: $Ln_2Te_5$ > $U_2Te_5$ > $Np_2Se_5$ > $Th_2Se_5$ > $Th_2S_5$ > $Np_2O_5$, consistent with the general trend observed for tellurides, selenides, sulfides, and oxides. This difference in the tendencies among chalcogens to engage in chalcogen–chalcogen interactions has been mainly attributed to the different degree of s-p mixing.[5] Strong s-p mixing for lighter main-group elements favors a Peierls distortion to form insulating discrete oligomers and monomers, as in $Th_2Se_5$, $Th_2S_5$, and $Np_2O_5$. In contrast, heavier main-group elements have weaker s-p mixing owing to the contraction of less-screened s orbitals, which allows the existence of less distorted, more metallic entities such as linear chains and planar sheets, as in $Ln_2Te_5$, $U_2Te_5$, and $Np_2Se_5$. The linear chain in $Np_2Se_5$ can be considered to result from a minor Peierls distortion of an equally spaced chalcogenide chain, compared to the more complete distortion seen in $Th_2S_5$ and $Th_2Se_5$. Alternatively this effect can be understood from the difference in chalcogenide basicity and polarizability; the heavier main-group elements, such as Te, are more basic and softer than the


dx.doi.org/10.1021/ic401384t | Inorg. Chem. 2013, 52, 9111–9118

light element O. Therefore, the electrons on the Te atoms are easier to delocalize into neighboring Te atoms.

Both the susceptibility to the Peierls distortion and the extent of Q−Q bonding depend on the electron count in the anion entities, which is determined by the redox chemistry between the metal and chalcogen (M−Q interactions).[5] The electronic structures of $AAn_2Q_6$ compounds have been explained by the insertion of electrons from metals to the Q p $\sigma^*$ orbitals into the lowest unoccupied molecular orbital (LUMO).[45,49] A similar qualitative argument may provide insight into the different Q−Q interactions observed for $M_2Q_5$ as well. The relative $M^{4+}$ standard reduction potentials ($E^\circ$) in aqueous solutions under acidic conditions decrease in the order of Nd (+4.9 V) > Np (+0.22(1) V) > U (−0.553(4) V) > Th (−3.8 V) as a result of a delocalization of f electrons.[69,70] Whereas these potentials are not expected to be reproduced in the solid-state chalcogenides discussed here, their trend suggests that among the $M^{3+}$ cations, $Ln^{3+}$ is the least susceptible toward the loss of electrons whereas $Th^{3+}$ is the most susceptible when surrounded by the same chalcogen in a similar coordination environment; the oxidizing abilities of chalcogen increase in the order of Te < Se < S < O. Therefore, the number of electrons provided by the metal to the Q p $\sigma^*$ orbitals of the chalcogenide network should increase across the series from $Ln_2Te_5$, $U_2Te_5$, $Np_2Se_5$, $Th_2Se_5$, $Th_2S_5$, to $Np_2O_5$. As a result, the chalcogenides sublattices are gradually broken down from a two-dimensional Te network in $Ln_2Te_5$, to one-dimensional chains in $U_2Te_5$ and $Np_2Se_5$, to Se oligomers in $Th_2Se_5$, to $S_2^{2-}$ dimers and $S^{2-}$ anions in $Th_2S_5$, to discrete $O^{2-}$ anions in $Np_2O_5$.

Besides the Q−Q and M−Q interactions, it has been suggested that the size ratio of metal to chalcogen could influence overall electronic structures of these compounds.[67] The crystal radii for six-coordinate ions are $Np^{3+}$= 1.15 Å, $Np^{4+}$ = 1.01 Å, $Th^{4+}$ = 1.08 Å, $Se^{2-}$ = 1.84 Å, and $S^{2-}$ = 1.70 Å.[71] Low metal:chalcogen radii ratios favor more Q−Q interactions, as larger cations tend to break the contacts between chalcogen atoms. Considering the rigid three-dimensional structures of connected metal polyhedra, steric effects could be significant in $Np_2Se_5$, $Th_2Se_5$, and $Th_2S_5$. In fact, we are unable to distinguish definitively the potentially complementary roles played by steric versus electronic effects when comparing the nonmodulated structures of $Np_2Se_5$ and $Th_2S_5$ to the modulated structure of $Th_2Se_5$.

## CONCLUSIONS

The crystal structure and electronic properties of $Np_2Se_5$ have been reinvestigated using single-crystal X-ray diffraction methods, XANES, and magnetic susceptibility measurements. Our studies have shown $Np_2Se_5$ to have a highly related but different structure from those of $Th_2S_5$ and $Th_2Se_5$. The results are discussed in terms of a Np valence state between +3 and +4. The major evidence in support of this interpretation lies in the chalcogenide sublattice, where the corresponding linear Se chains in $Np_2Se_5$ distort into Se oligomers in $Th_2Se_5$ and further into discrete $S_2^{2-}$ and $S^{2-}$ anions in $Th_2S_5$. These structural and chemical differences have been attributed to different Q−Q and M−Q interactions, and size ratios of metal to chalcogen. Overall, the electronic properties of $Np_2Se_5$ fit into the general trend observed for those of the $M_2Q_5$ series. $Np_2Se_5$ provides an example of the vital role played by Np in studies of actinide chalcogenide chemistry, the result of its varying redox chemistry.

## ASSOCIATED CONTENT

### Supporting Information

Crystallographic file in cif format for $Np_2Se_5$. This material is available free of charge via the Internet at http://pubs.acs.org.

## AUTHOR INFORMATION

### Corresponding Author

*E-mail: gjin@anl.gov.

### Notes

The authors declare no competing financial interest.

## ACKNOWLEDGMENTS

The research at Argonne National Laboratory was supported by the U.S. Department of Energy, Basic Energy Sciences, Chemical Sciences, Biosciences, under contract DEAC02-06CH11357. X-ray absorption spectroscopy data were obtained at the Advanced Photon Source, which is supported by the U.S. DOE, OBES, Materials Sciences under the same contract number. The work at Northwestern University was supported by the U.S. Department of Energy, Basic Energy Sciences, Chemical Sciences, Biosciences, and Geosciences Division and Division of Materials Sciences and Engineering Grant ER-15522.

## REFERENCES

(1) *The Chemistry of the Actinide and Transactinide Elements*, 3rd ed.; Morss, L. R., Edelstein, N. M., Fuger, J., Katz, J. J., Eds.; Springer: Dordrecht, The Netherlands, 2006.
(2) Lee, S.; Foran, B. J. *J. Am. Chem. Soc.* **1996**, *118*, 9139−9147.
(3) Chung, D.-Y.; Jobic, S.; Hogan, T.; Kannewurf, C. R.; Brec, R.; Rouxel, J.; Kanatzidis, M. G. *J. Am. Chem. Soc.* **1997**, *119*, 2505−2515.
(4) Choi, K.-S.; Patschke, R.; Billinge, S. J. L.; Waner, M. J.; Dantus, M.; Kanatzidis, M. G. *J. Am. Chem. Soc.* **1998**, *120*, 10706−10714.
(5) A. Papoian, G.; Hoffmann, R. *Angew. Chem., Int. Ed.* **2000**, *39*, 2408−2448.
(6) Malliakas, C.; Billinge, S. J. L.; Kim, H. J.; Kanatzidis, M. G. *J. Am. Chem. Soc.* **2005**, *127*, 6510−6511.
(7) Graf, C.; Assoud, A.; Mayasree, O.; Kleinke, H. *Molecules* **2009**, *14*, 3115−3131.
(8) Noel, H. *J. Solid State Chem.* **1984**, *52*, 203−210.
(9) Yoshida, Z.; Johnson, S. G.; Kimura, T.; Krsul, J. R. In *The Chemistry of the Actinide and Transactinide Elements*, 3rd ed.; Morss, L. R., Edelstein, N. M., Fuger, J., Katz, J. J., Eds.; Springer: Dordrecht, The Netherlands, 2006; Vol. 2, pp 699−812.
(10) Jin, G. B.; Skanthakumar, S.; Haire, R. G.; Soderholm, L.; Ibers, J. A. *Inorg. Chem.* **2011**, *50*, 1084−1088.
(11) Thevenin, T.; Jove, J.; Pages, M. *Hyperfine Interact.* **1984**, *20*, 173−186.
(12) Marcon, J.-P. *C. R. Acad. Sc. Paris, Ser. C* **1967**, *265*, 235−237.
(13) Thévenin, T.; Pagès, M.; Wojakowski, A. *J. Less-Common Met.* **1982**, *84*, 133−137.
(14) Marcon, J.-P. *Commis. Energ. At. [Fr], Rapp. CEA-R-3919* **1969**, 1−99.
(15) Damien, D.; Damien, N.; Charvillat, J. P.; Jove, J. *Inorg. Nucl. Chem. Lett.* **1973**, *9*, 649−655.
(16) Bellott, B. J.; Haire, R. G.; Ibers, J. A. *Z. Anorg. Allg. Chem.* **2012**, *638*, 1777−1779.
(17) Damien, D. *J. Inorg. Nucl. Chem.* **1974**, *36*, 307−308.
(18) Ulrich, B. *J. Less-Common Met.* **1987**, *128*, 7−45.
(19) Graham, J.; McTaggart, F. K. *Aust. J. Chem.* **1960**, *13*, 67−73.
(20) Noel, H. *J. Inorg. Nucl. Chem.* **1980**, *42*, 1715−1717.
(21) Noel, H.; Potel, M. *Acta Crystallogr., Sect. B: Struct. Commun.* **1982**, *38*, 2444−2445.
(22) Kohlmann, H.; Beck, H. P. *Z. Kristallogr.* **1999**, *214*, 341−345.
(23) Bellott, B. J.; Malliakas, C. D.; Koscielski, L. A.; Kanatzidis, M. G.; Ibers, J. A. *Inorg. Chem.* **2012**, *52*, 944−949.

(24) Tougait, O.; Potel, M.; Padiou, J.; Noël, H. *J. Alloys Compd.* **1997**, *262*−*263*, 320−324.
(25) Stowe, K. *J. Alloys Compd.* **1997**, *246*, 111−123.
(26) Jin, G. B.; Choi, E. S.; Guertin, R. P.; Brooks, J. S.; Booth, C. H.; Albrecht-Schmitt, T. E. *Inorg. Chem.* **2007**, *46*, 9213−9220.
(27) Wells, D. M.; Jin, G. B.; Skanthakumar, S.; Haire, R. G.; Soderholm, L.; Ibers, J. A. *Inorg. Chem.* **2009**, *48*, 11513−11517.
(28) Tideswell, N. W.; Kruse, F. H.; McCullough, J. D. *Acta Crystallogr.* **1957**, *10*, 99−102.
(29) *APEX2 Version 2009.5-1 and SAINT Version 7.34a Data Collection and Processing Software*; Bruker Analytical X-Ray Instruments, Inc.: Madison, WI, 2009.
(30) *SMART Version 5.054 Data Collection and SAINT-Plus Version 6.45a Data Processing Software for the SMART System*; Bruker Analytical X-Ray Instruments, Inc.: Madison, WI, 2003.
(31) Sheldrick, G. M. *Acta Crystallogr., Sect. A: Found. Crystallogr.* **2008**, *64*, 112−122.
(32) Gelato, L. M.; Parthé, E. *J. Appl. Crystallogr.* **1987**, *20*, 139−143.
(33) McMaster, W. H.; Del Grande, N. K.; Mallett, J. H.; Hubbell, J. H. *Compilation of X-ray cross sections*; Lawrence Livermore National Laboratory: Livermore, CA, 1970.
(34) Teo, B. K. *EXAFS: basic principles and data analysis*; Springer-Verlag: Berlin, Germany, 1986.
(35) Webb, S. M. *Phys. Scr.* **2005**, *T115*, 1011−1014.
(36) Newville, M. *J. Synchrotron Rad.* **2001**, *8*, 322−324.
(37) Marchand, P.; Marmet, L. *Rev. Sci. Instrum.* **1983**, *54*, 1034−1041.
(38) Jin, G. B.; Skanthakumar, S.; Soderholm, L.; Ibers, J. A., unpublished results.
(39) Koscielski, L. A.; Bellott, B.; Ibers, J. A., unpublished results.
(40) Jin, G. B.; Choi, E. S.; Albrecht-Schmitt, T. E. *J. Solid State Chem.* **2009**, *182*, 1075−1081.
(41) Jin, G. B.; Choi, E. S.; Guertin, R. P.; Albrecht-Schmitt, T. E. *J. Solid State Chem.* **2008**, *181*, 14−19.
(42) Bugaris, D. E.; Copping, R.; Tyliszczak, T.; Shuh, D. K.; Ibers, J. A. *Inorg. Chem.* **2010**, *49*, 2568−2575.
(43) Wells, D. M.; Skanthakumar, S.; Soderholm, L.; Ibers, J. A. *Acta Crystallogr., Sect. E: Struct. Rep. Online* **2009**, *65*, i14.
(44) Jin, G. B.; Raw, A. D.; Skanthakumar, S.; Haire, R. G.; Soderholm, L.; Ibers, J. A. *J. Solid State Chem.* **2010**, *183*, 547−550.
(45) Bugaris, D. E.; Wells, D. M.; Yao, J.; Skanthakumar, S.; Haire, R. G.; Soderholm, L.; Ibers, J. A. *Inorg. Chem.* **2010**, *49*, 8381−8388.
(46) Bensalem, A.; Meerschaut, A.; Rouxel, J. *C. R. Acad. Sci. Ser. II* **1984**, *299*, 617−619.
(47) Chauvin, R. *J. Phys. Chem.* **1992**, *96*, 9194−9197.
(48) Chan, B. C.; Hulvey, Z.; Abney, K. D.; Dorhout, P. K. *Inorg. Chem.* **2004**, *43*, 2453−2455.
(49) Mizoguchi, H.; Gray, D.; Huang, F. Q.; Ibers, J. A. *Inorg. Chem.* **2006**, *45*, 3307−3311.
(50) Denecke, M. A.; Dardenne, K.; Marquardt, C. M. *Talanta* **2005**, *65*, 1008−1014.
(51) Deslattes, R. D.; Kessler, E. G.; Indelicato, P.; de Billy, L.; Lindroth, E.; Anton, J. *Rev. Mod. Phys.* **2003**, *75*, 35−99.
(52) Soderholm, L.; Antonio, M. R.; Williams, C.; Wasserman, S. R. *Anal. Chem.* **1999**, *71*, 4622−4628.
(53) Conradson, S. D.; Abney, K. D.; Begg, B. D.; Brady, E. D.; Clark, D. L.; den Auwer, C.; Ding, M.; Dorhout, P. K.; Espinosa-Faller, F. J.; Gordon, P. L.; Haire, R. G.; Hess, N. J.; Hess, R. F.; Keogh, D. W.; Lander, G. H.; Lupinetti, A. J.; Morales, L. A.; Neu, M. P.; Palmer, P. D.; Paviet-Hartmann, P.; Reilly, S. D.; Runde, W. H.; Tait, C. D.; Veirs, D. K.; Wastin, F. *Inorg. Chem.* **2004**, *43*, 116−131.
(54) Antonio, M. R.; Soderholm, L. In *The Chemistry of the Actinide and Transactinide Elements*, 3rd ed.; Morss, L. R., Edelstein, N. M., Fuger, J., Katz, J. J., Eds.; Springer: Dordrech The Netherlandst, 2006; Vol. *5*, pp 3086−3198.
(55) Schelter, E. J.; Wu, R.; Veauthier, J. M.; Bauer, E. D.; Booth, C. H.; Thomson, R. K.; Graves, C. R.; John, K. D.; Scott, B. L.; Thompson, J. D.; Morris, D. E.; Kiplinger, J. L. *Inorg. Chem.* **2010**, *49*, 1995−2007.
(56) Kalkowski, G.; Kaindl, G.; Bertram, S.; Schmiester, G.; Rebizant, J.; Spirlet, J. C.; Vogt, O. *Solid State Commun.* **1987**, *64*, 193−196.
(57) Kalkowski, G.; Kaindl, G.; Brewer, W. D.; Krone, W. *Phys. Rev. B* **1987**, *35*, 2667−2677.
(58) Allen, P. G.; Bucher, J. J.; Shuh, D. K.; Edelstein, N. M.; Reich, T. *Inorg. Chem.* **1997**, *36*, 4676−4683.
(59) Staub, U.; Soderholm, L. In *Handbook on the Physics and Chemistry of Rare Earths*; Karl .A., Gschneidner, J. L. E., Maple, M. B., Eds.; Elsevier: Amsterdam, The Netherlands, 2000; Vol. *30*, pp 491−545.
(60) Maple, M. B.; Wohlleben, D. *Phys. Rev. Lett.* **1971**, *27*, 511−515.
(61) Soderholm, L.; Antonio, M. R.; Skanthakumar, S.; Williams, C. W. *J. Am. Chem. Soc.* **2002**, *124*, 7290−7291.
(62) Morosan, E.; Natelson, D.; Nevidomskyy, A. H.; Si, Q. *Adv. Mater.* **2012**, *24*, 4896−4923.
(63) Brese, N. E.; O'Keeffe, M. *Acta Crystallogr., Sect. B* **1991**, *47*, 192−197.
(64) Jin, G. B.; Skanthakumar, S.; Haire, R. G.; Soderholm, L.; Ibers, J. A. *Inorg. Chem.* **2011**, *50*, 9688−9695.
(65) Fulde, P. *Electron Correlations in Molecules and Solids*; Springer-Verlag GmbH: Berlin, Germany, 1995.
(66) Pardo, M. P.; Flahaut, J. *Bull. Soc. Chim. Fr.* **1967**, 3658−3664.
(67) DiMasi, E.; Foran, B.; Aronson, M. C.; Lee, S. *Chem. Mater.* **1994**, *6*, 1867−1874.
(68) Forbes, T. Z.; Burns, P. C.; Skanthakumar, S.; Soderholm, L. *J. Am. Chem. Soc.* **2007**, *129*, 2760−2761.
(69) Morss, L. R. In *Standard Potentials in Aqueous Solutions*; Bard, A. J., Parsons, R., Jordan, J., Eds.; IUPAC (Marcel Dekker): New York, 1985; pp 587−629.
(70) Konings, R. J. M.; Morss, L. R.; Fuger, J. In *The Chemistry of the Actinide and Transactinide Elements*, 3rd ed.; Morss, L. R., Edelstein, N. M., Fuger, J., Katz, J. J., Eds.; Springer: Dordrech, The Netherlandst, 2006; Vol. *4*, pp 2113−2224.
(71) Shannon, R. *Acta Crystallogr., Sect. A* **1976**, *32*, 751−767.